

Nanometer-Scale Permeabilization and Osmotic Swelling Induced by 5-ns Pulsed Electric Fields

Esin B. Sözer¹ · Yu-Hsuan Wu² · Stefania Romeo³ · P. Thomas Vernier¹

Received: 29 January 2016 / Accepted: 11 July 2016 / Published online: 19 July 2016
© Springer Science+Business Media New York 2016

Abstract High-intensity nanosecond pulsed electric fields (nsPEFs) permeabilize cell membranes. Although progress has been made toward an understanding of the mechanism of nsPEF-induced membrane poration, the dependence of pore size and distribution on pulse duration, strength, number, and repetition rate remains poorly defined experimentally. In this paper, we characterize the size of nsPEF-induced pores in living cell membranes by isosmotically replacing the solutes in pulsing media with polyethylene glycols and sugars before exposing Jurkat T lymphoblasts to 5 ns, 10 MV/m electric pulses. Pore size was evaluated by analyzing cell volume changes resulting from the permeation of osmolytes through the plasma membrane. We find that pores created by 5 ns pulses have a diameter between 0.7 and 0.9 nm at pulse counts up to 100 with a repetition rate of 1 kHz. For larger number of pulses, either the pore diameter or the number of pores created, or both, increase with increasing pulse counts. But the prevention of cell swelling by PEG 1000 even after 2000 pulses suggests that 5 ns, 10 MV/m pulses cannot produce pores with a diameter larger than 1.9 nm.

Keywords Nanosecond pulsed electric field · Osmotic swelling · Electroporation/electropermeabilization

Introduction

High-intensity, nanosecond-to-submicrosecond pulse exposures, sometimes called nanosecond pulsed electric fields (nsPEFs) have been shown to be versatile, nondestructive stimuli capable of producing a variety of specific cellular responses such as membrane permeabilization and intracellular calcium release (Vernier et al. 2003, 2006), cellular apoptosis for tumor shrinking (Beebe et al. 2004; Nuccitelli et al. 2009; Rubinsky 2007; Garon et al. 2007), temporary blockage of action potential propagation in nerves (Rogers et al. 2004), catecholamine secretion (Craviso et al. 2009), activation of platelets, and release of growth factors for accelerated wound healing (Schoenbach et al. 2007; Zhang et al. 2008). Cell membrane permeabilization caused by nsPEFs (nanoelectroporation) is believed to involve the formation of hydrophilic pores in lipid bilayers through a process that is strongly dependent on the applied field intensity and on the pulse duration (Levine and Vernier 2010), as is the permeabilization associated with pulses of microsecond or millisecond duration (Zimmermann 1982), although the details of the physical mechanisms may be different. Until the nature of the pore structure and the details of the mechanisms that govern pore size and lifetime are better understood, the practical utilization of nsPEF-induced electropermeabilization in biomedical and biotechnological applications, with the potential for greater energy efficiency and less invasive procedures, will be ad hoc and empirical.

Membrane permeabilization is traditionally detected by measuring the uptake of fluorescent dyes like propidium or YO-PRO-1 that cannot pass through an intact membrane,

✉ Esin B. Sözer
esozer@odu.edu

¹ Frank Reidy Research Center for Bioelectrics, Old Dominion University, 4211 Monarch Way, STE 300, Norfolk, VA, USA

² Mork Family Department of Chemical Engineering and Materials Science, Viterbi School of Engineering, University of Southern California, Los Angeles, CA, USA

³ CNR - Institute for Electromagnetic Sensing of the Environment (IREA), Via Diocleziano 328, 80124 Naples, Italy

and this method has been used in studies of permeabilization by nanosecond (Vernier et al. 2006; Napotnik et al. 2012) and submicrosecond pulses (Bowman et al. 2010). The results of those studies are consistent with models of electroporation by nanosecond (Smith and Weaver 2011) or longer pulses (Bilska et al. 2000; DeBruin and Krassowska 1999) and experiments (Pakhomov et al. 2009) indicating that membrane electropore diameters fall roughly in the range 0.8–1.5 nm. Note that these reports conceptualize permeabilizing structures as pores, similar to those observed in molecular dynamics simulations (Levine and Vernier 2010), although their precise biomolecular composition is unknown.

Quantification of membrane permeabilization based on influx of fluorescent dyes, however, is limited by dye excitation and emission efficiency, and detector sensitivity. Measurement of cell volume changes arising from colloidal osmotic imbalance was introduced as a method to control and study electroporation induced by microsecond pulses (Kinosita and Tsong 1977; Golzio et al. 1998; Claessens et al. 2008), and has been recently proven to be a more sensitive method for characterizing nsPEF-induced plasma membrane permeabilization as well (André et al. 2010; Nesin et al. 2011).

When the cell membrane is permeabilized, small intracellular and extracellular solutes (Na^+ , K^+ , Cl^- , Ca^{2+} , etc.) can pass freely through the membrane, causing a loss of the concentration gradients maintained by living cells. Larger intracellular solutes (polypeptides, polynucleotides, polysaccharides, etc.) cannot pass through the permeabilized membrane, creating an osmotic imbalance. In the general case, the osmotic pressure resulted from the trapped intracellular colloidal solutes leads to water influx from the extracellular medium and an increase in cell volume (André et al. 2010; Nesin et al. 2011).

Multiple studies have shown that cell swelling can be suppressed or reversed (cell shrinking) if the extracellular medium contains appropriate concentrations of large solutes which cannot pass through the permeabilized membrane, thus counterbalancing the intracellular colloid osmotic pressure (Kinosita and Tsong 1977; Sabirov and Okada 2004; Sukhorukov et al. 2009; Saulis et al. 1991). The average size of molecules whose transport is mediated by permeabilizing structures can be estimated using this method, by isosmotically replacing smaller extracellular solutes with sugars and larger molecules of various sizes (Nesin et al. 2011). For simplicity, we will refer to these measurements as pore size estimates.

In the present work, we employed polyethylene glycol (PEG) and two sugars of different sizes to estimate the pore size created in Jurkat T lymphoblast cell membranes by nsPEF exposure. The pulse duration in this study is 5 ns, considerably shorter than the pulses investigated in other

studies. In addition, we examined the dependence of pore size on pulse parameters, especially the number of pulses.

Materials and Methods

Cell Culture

Jurkat T lymphoblasts (ATCC TIB-152, Manassas, VA) were grown in RPMI 1640 (Mediatech, Manassas, VA) containing 10 % heat-inactivated fetal bovine serum (Gibco, Carlsbad, CA), 2 mM L-glutamine (Gibco), 50 units/mL penicillin (Gibco), and 50 $\mu\text{g}/\text{mL}$ streptomycin (Gibco). Cells were maintained in exponential growth at 37 °C in a humidified, 5 % CO_2 atmosphere.

Cell Preparation

For pulse treatment, cells were centrifuged and resuspended at 1×10^6 cells/mL in different pulsing media at room temperature. Description of media can be found in the section “[Chemicals and pulsing media](#).” In most of the experiments, cells were loaded with 0.5 μM calcein-AM in RPMI 1640 for 15 min before suspending in different pulsing media. Calcein fluorescence was used to facilitate identification of the perimeter of the cell, but quantitative image analysis was carried out only with DIC images.

Chemicals and Pulsing Media

The reference medium for measuring nsPEF effects on cell volume (extracted from the cross-sectional area) was RPMI 1640, the medium used for culturing the cells. The osmolality of RPMI 1640 measured in our lab is ~ 280 mOsm/kg. For sugar test solutions, each with total osmolality approximately 280 mOsm/kg, D-myo-inositol (Fisher) and sucrose (Fisher) were combined with RPMI 1640 and water for final osmolalities of 116 mOsm/kg inositol, and 116, 150, and 200 mOsm/kg sucrose. In experiments with PEG, media were formulated similarly. Because the osmotic properties of large PEGs depend on their molecular size and concentration, isosmotic PEG 1000 (Polysciences, Inc.) concentrations were found by trial and error (Sabirov and Okada 2004; Sukhorukov et al. 2009). 50, 116, 150, and 200 mOsm/kg PEG 1000 in RPMI solutions were prepared. The final osmolality of each solution was measured with a vapor pressure osmometer (Wescor Inc., Utah). The final osmolality of all solutions was between 280 and 300 mOsm/kg.

Inositol and sucrose molecular structures were represented and analyzed using the software package visual molecular dynamics (VMD). Molecular structures and three-dimensional representations of the minimum

geometric cross sections based on van der Waal radii are shown in Fig. 1. Minimum molecular diameters were measured from the structure planes with the smallest cross sections (Fig. 1). The smallest circle accommodating the smaller two of the three Cartesian diameters was used to determine the minimum cross-sectional diameter (Nesin et al. 2011). The hydrodynamic radius of a PEG random coil depends on its molecular weight and the solution viscosity through the Einstein viscosity relation (Kuga 1981; Armstrong et al. 2004). The hydrodynamic diameter of PEG 1000 presented in this study is 1.9 nm, based on its viscosity in Ringer's solution (Sabirov and Okada 2004).

Nanosecond Pulsed Electric Field Exposures

A tungsten wire electrode delivery system for exposure of cells to nanosecond pulsed electric fields on a microscope stage was previously described (Wu et al. 2013). The separation of the two 100 μm diameter parallel wires is 200 μm center-to-center (100 μm between the closest tangential points on the two electrodes). A resonant-charged, solid-state, Marx-bank-driven, hybrid-core compression, diode-opening switch pulse generator, designed and assembled at the University of Southern California (Sanders et al. 2009), delivered 5 ns, 10 MV/m electric pulses at a 1 kHz repetition rate to the electrodes immersed in cell suspensions in ambient atmosphere at room temperature. The pulse has a 4-ns rise time (10–90 %), 5.3-ns full-width at half-maximum.

For microscopic observation of cells before, during, and after nsPEF exposure, an 8-well coverglass chamber was placed on the microscope stage. 200 μL of 1×10^6 cells/mL were added to a chamber followed by carefully

positioning the electrodes, until they contact the bottom of the well using a micromanipulator (MP-225, Sutter). Cells were allowed to settle and adhere to the chamber floor for 10–15 min before nsPEF exposure (Wu et al. 2013). All experiments were performed at room temperature. Details of the experimental setup including a schematic of the whole system can be found in Wu et al. 2013.

Microscopy and Image Analysis

Observations of live cells were made using a Zeiss (Göttingen, Germany) Axiovert 200 epifluorescence microscope with 63 \times water immersion objective and ImageEM EM-CCD camera (Hamamatsu, Japan). Images of cells were taken immediately before and at various times (10 s to 5 min) after nsPEF exposure. Captured images were analyzed with Hamamatsu SimplePCI and ImageJ (<http://imagej.nih.gov/ij/>) software. To reduce variability, only cells in the center of the exposure chamber and at least 5 μm from the electrode surfaces were tracked and analyzed to insure a uniform electric field exposure (Wu et al. 2013). The cell perimeter was traced in DIC images using a freehand selection function, and then the cell cross-section area defined by the drawn perimeter was determined by the software ImageJ (<http://imagej.nih.gov/ij/>). Cell cross-section area (A) at different time points was normalized to the area before pulsing (A_0), where $A_{\text{normalized}} = A/A_0$. For each pulsing condition, at least three experiments were carried out, and a total of at least 60 cells (n) were analyzed. Pooled data are given as mean \pm SE (standard error of the mean) of experiments. SE is defined as standard deviation divided by the square root of the number of cells analyzed (n) in each experiment. If the SE value is smaller

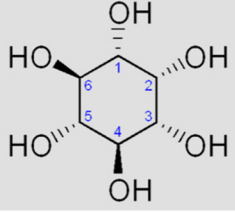
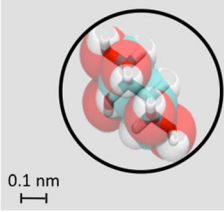
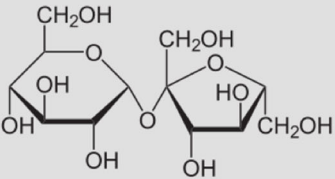
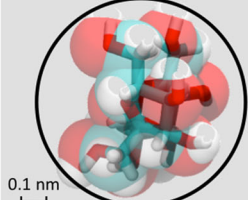
Molecules	Chemical Structure	3-D Molecular Views	Minimum Cross Sectional Diameter
<i>Inositol</i>			0.7 nm
<i>Sucrose</i>			0.9 nm

Fig. 1 Molecular structures and minimum cross-sectional diameters of inositol and sucrose

than the size of symbol, the error bar may not be seen in the graph.

Results

Cell Volume Changes Induced by Nanosecond Pulsed Electric Fields (nsPEFs)

Cell swelling (increase in cell volume) after nsPEF treatment has been shown to indicate plasma membrane permeabilization for pulses lasting 60 ns or longer (André et al. 2010; Nesin et al. 2011). Previously, we demonstrated that a single pulse even as short as 5 ns produces volume increases in Jurkat cells, consistent with colloidal osmotic swelling (Romeo et al. 2013). Figure 2 shows a representative series of images of a single cell before and up to 5 min after exposure to 10 pulses, 5 ns, 10 MV/m delivered at 1 kHz in RPMI 1640 medium. The cross-sectional areas of the cell extracted from these images are listed in Table 1.

The extent of swelling is a function of the number of pulses delivered. The cross-sectional area change (from which an approximation of the volume change can be extracted) after nsPEF treatment increases with increasing pulse count (Fig. 3). Five minutes after exposure to 30 pulses, 5 ns, the area has increased by a factor of 1.6 (two-fold volume increase, assuming spherical geometry). Note that 10 and 20 pulses induce the same extent of cell

swelling, at least after the first 180 s. This suggests that these two pulsing conditions induce, quantitatively and/or qualitatively, similar “pore” populations and thus similar swelling, under our experimental conditions. Taken together with our earlier report of influx of the normally impermeant fluorescent dye YO-PRO-1 after similar pulse doses (Vernier et al. 2006), these images and data support the interpretation that cell swelling after exposure to 5 ns, 10 MV/m electric pulses is a dose-dependent indicator of pulse-induced, plasma membrane permeabilization.

Impermeant Solute Blocks Cell Swelling (PEG 1000)

To investigate further the colloidal osmotic swelling in cells permeabilized with 5 ns pulses, we compared volume changes in cells suspended in isosmotic solutions containing the large molecule PEG 1000 at several osmolalities. Figure 4 shows the swelling response of Jurkat cells exposed to 30 pulses, 10 MV/m at 1 kHz in isosmotic RPMI 1640 solutions containing 50–150 mOsm/kg PEG 1000. Note that swelling induced in 50 mOsm/kg PEG 1000 (Fig. 4a) is less than that in standard RPMI (Fig. 3, 30 p). This is expected due to the large PEG 1000 molecules partially balancing the contribution of large solutes to the intracellular osmolality. Swelling is completely blocked when the extracellular osmolality of large molecules at the time of pulse exposure is sufficiently high to completely balance the intracellular large molecule osmolality. Swelling induced by 30 pulses, 5 ns is blocked by

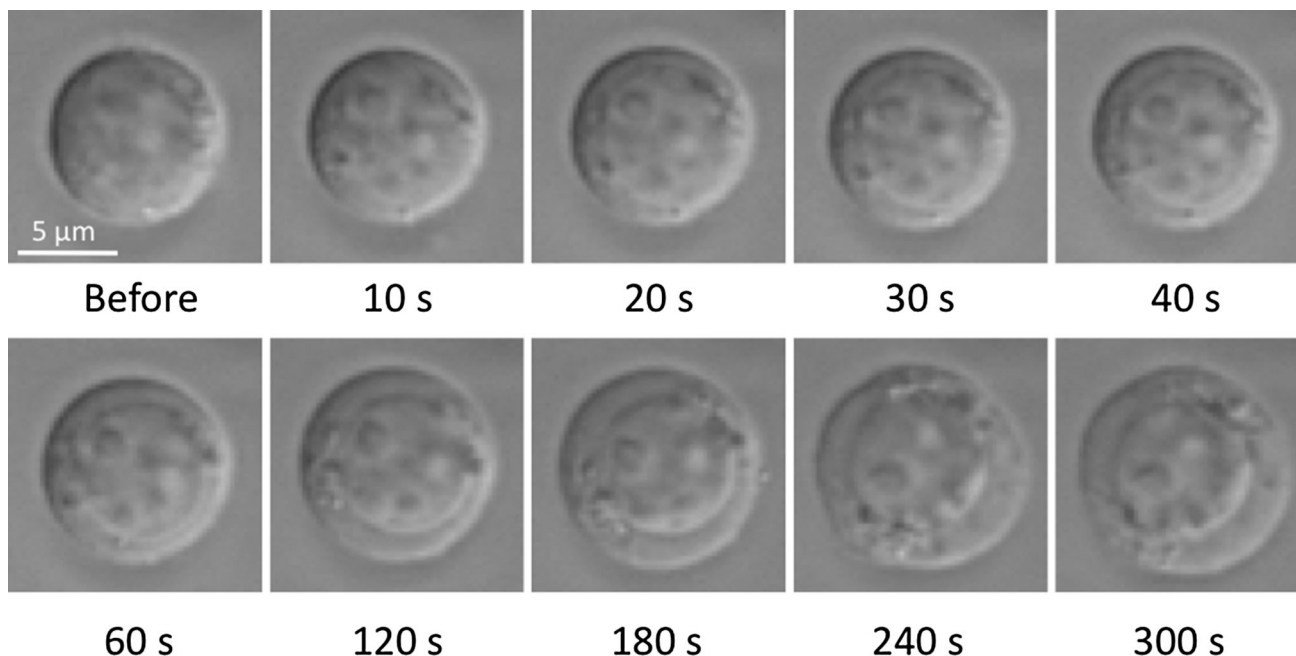
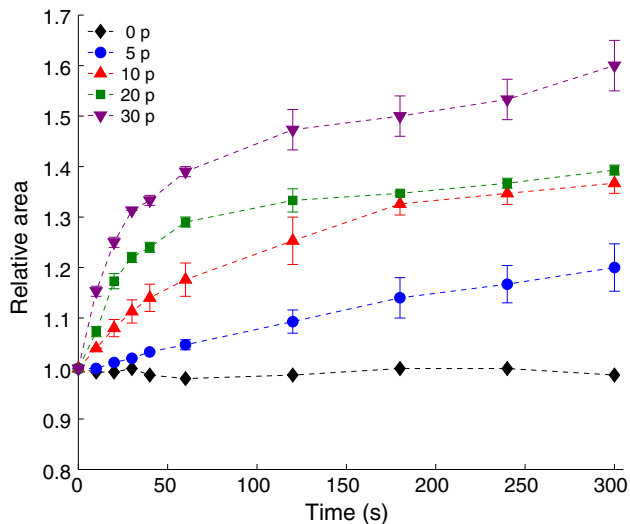


Fig. 2 Time series of DIC images showing a Jurkat cell swelling after nsPEF exposure (10 pulses, 5 ns, 10 MV/m at 1 kHz) in RPMI 1640. Scale bar is 5 μ m

Table 1 Cross-sectional area of a representative Jurkat cell after nsPEF exposure (10 pulses, 5 ns, 10 MV/m at 1 kHz). Values were extracted from the images in Fig. 2

Time (s)	0	10	20	30	40	60	120	180	240	300
Area (μm^2)	72.4	74.3	78.4	78.6	84.1	85.6	94.4	97.8	108	108

**Fig. 3** Dose-dependent area increase of Jurkat cells after nsPEF exposure to 0, 5, 10, 20, and 30 electric pulses, 5 ns delivered with 10 MV/m field strength and a repetition rate of 1 kHz in RPMI 1640. Increasing the number of pulses delivered results in increased swelling. Results are presented as mean \pm SE for at least 60 cells from at least three independent experiments for each pulsing condition at 25 °C

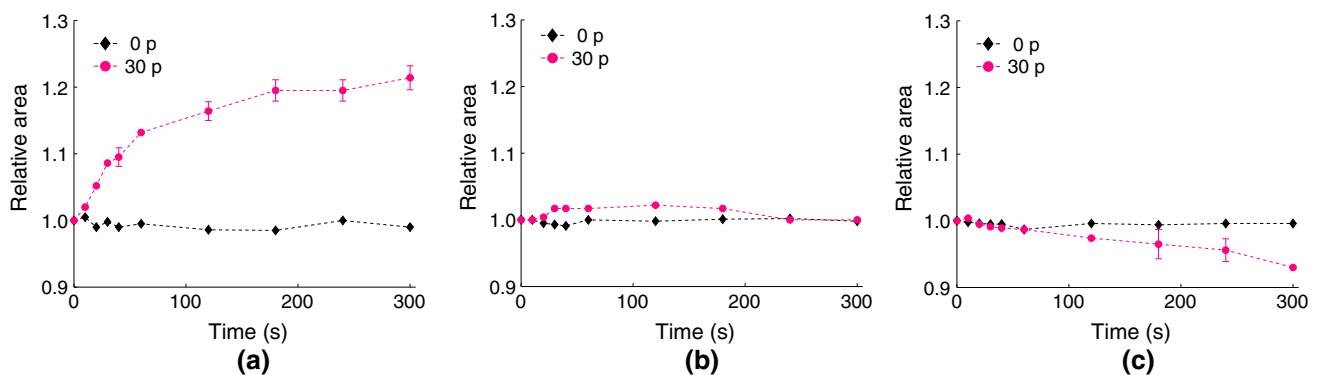
116 mOsm/kg PEG 1000. At higher osmolalities of PEG 1000, the cells shrink after pulse treatment, consistent with observations reported for significantly longer pulses (Nesin et al. 2011). In sham exposures, cell volume did not change during the 5-min observation period, demonstrating that

osmoregulatory mechanisms are not affected by PEG 1000 in the medium over this time period.

These results suggest that PEG 1000 does not penetrate into cells exposed to the 5-ns pulse doses used in these experiments and that the osmolality of the large intracellular solutes that contribute to colloidal osmotic swelling is <150 mOsm/kg. In subsequent experiments we used 116 mOsm/kg of the external solute, which provides an approximately osmotically balanced condition (no swelling or shrinking with PEG 1000) in suspensions of 5-ns pulse-permeabilized Jurkat cells.

Cell Swelling Inhibited by Inositol, Blocked by Sucrose

To compare the effects of solutes smaller than PEG 1000 on cell volume changes triggered by 5 ns, 10 MV/m pulses, we treated cells in RPMI medium containing either 116 mOsm/kg inositol or sucrose as described in “Materials and Methods” section (Fig. 5). In contrast to the significant volume increases observed in standard RPMI, cells in medium containing inositol showed less swelling, and sucrose blocked swelling completely. Partial blocking of swelling by inositol is probably a result of a small fraction of permeabilizing structures among the whole population that are impermeable to inositol molecules but permeable to solutes in standard RPMI that are smaller than inositol. In fact, at a low-dose exposure of 5 pulses, 10 MV/m, the swelling is completely blocked by

**Fig. 4** Inhibition of colloidal osmotic swelling in Jurkat cells by **a** 50 mOsm/kg, **b** 116 mOsm/kg, **c** 150 mOsm/kg of extracellular PEG 1000. Cells were exposed to 30 pulses, 5 ns, 10 MV/m, 1 kHz repetition rate. Higher osmolalities of PEG 1000 inhibit nsPEF-

induced cell swelling. Results are presented as mean \pm SE for at least 60 cells from at least three independent experiments for each pulsing condition at 25 °C

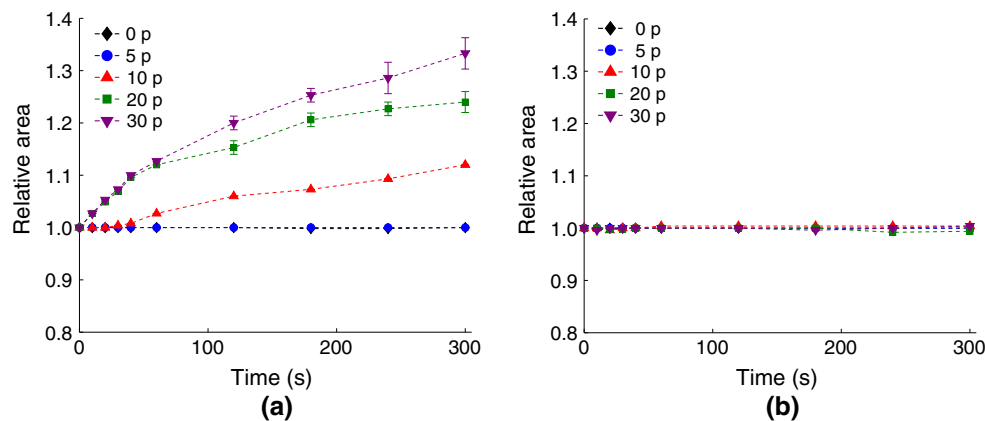


Fig. 5 Effect of 116 mOsm/kg **a** inositol and **b** sucrose on colloidal osmotic swelling in Jurkat cells permeabilized with 5 ns, 10 MV/m pulses delivered at 1 kHz. Inositol does not block swelling, but sucrose does, indicating that the smaller inositol molecule can pass

116 mOsm/kg inositol, indicating the absence of inositol-permeant structures. This is consistent with the dose-dependent nature of electric pulse-induced swelling observed with standard RPMI (Fig. 3).

Assuming that colloidal osmotic swelling is the mechanism underlying the observed volume increase, we can extract from these results an approximate size for the permeabilizing structures produced by 5-ns electric pulse exposure. For simplicity, we call these structures pores, although we emphasize that their precise nature has not been definitively established. When a molecule (inositol) is small enough to pass through the pores, it should not block swelling, because these molecules cannot offset the osmolality of the large impermeant molecules inside the cell. On the other hand, if the molecule (sucrose) is too large to pass through the pores and the sucrose osmolality is high enough, swelling will not occur, because the pre-pulse osmotic balance is maintained.

The minimum molecular cross-sectional diameters of inositol and sucrose are 0.7 and 0.9 nm, respectively. As shown in Fig. 5, inositol penetrates the nsPEF-permeabilized plasma membrane (swelling not blocked), but sucrose does not (swelling blocked). This evidence indicates that the diameter of pores created in the cell membrane by 5-ns pulsed electric fields is >0.7 and <0.9 nm, consistent with observations reported for significantly longer pulses (Nesin et al. 2011).

Pulse Dose and Pore Diameter

The increasing of swelling with increasing pulse count observed with inositol (Fig. 5) could be a result of an increasing number of pores or an increase in the diameter of pores, or some combination of these effects. To investigate whether increasing the number of pulses delivered

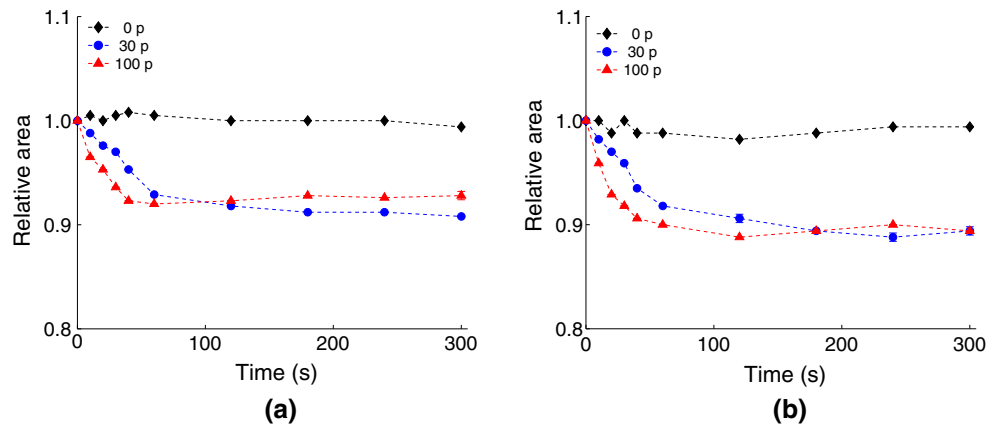
through the nanoelectropulse-induced permeabilizing structures (pores). Results are presented as mean \pm SE for at least 60 cells from at least three independent experiments for each pulsing condition at 25 °C

increases the diameter of the permeabilizing structures (pores), we increased the osmolality of sucrose to 150 and 200 mOsm/kg. At these higher concentrations, if the pores are large enough to permit sucrose transport, osmotic swelling should be observed, but if sucrose molecules cannot pass through the pores, the cells should shrink, as we observe with PEG 1000 (Fig. 4).

As seen in Fig. 6, cells in the suspensions with higher sucrose osmolalities shrink after 30 or even 100 pulses, 5 ns, with no volume recovery. These results imply that sucrose does not penetrate even into cells exposed to a large number of 5 ns pulses, or that the influx is minimal and thus does not produce a detectable volume change. We conclude that multiple pulses do not significantly increase the diameter of the permeabilizing structures beyond the 0.9 nm produced at lower pulse counts. These findings are in agreement with conclusions reported in Pakhomov et al. 2015 with 60 ns pulses. Also, Son and co-workers (Son et al. 2016), with completely different pulsing conditions (20 pulses, 100 μ s, 1 kV/cm, 1 Hz repetition rate), suggest that in a train of pulses, the first few pulses create a large number of pores, which exponentially decrease over time despite the applications of further pulses. The surviving pores tend to expand, but not enough to significantly increase the transport of small solutes like calcium. In spite of very different pulse widths, this numerical model is consistent with our observation that additional pulses do not create a significant population of large pores contributing to transport of larger molecules.

With PEG 1000, the response to 100 pulses is more complex. As expected, since the PEG 1000 molecule is about twice the size of sucrose (the hydrodynamic diameter of PEG 1000 is about 1.9 nm (Sabirov and Okada 2004), cell shrinking is observed after 100 pulses, 5 ns above 116 mOsm/kg (150 and 200 mOsm/kg; Fig. 7c, d) of PEG 1000, as it was for 30 pulses (Fig. 4).

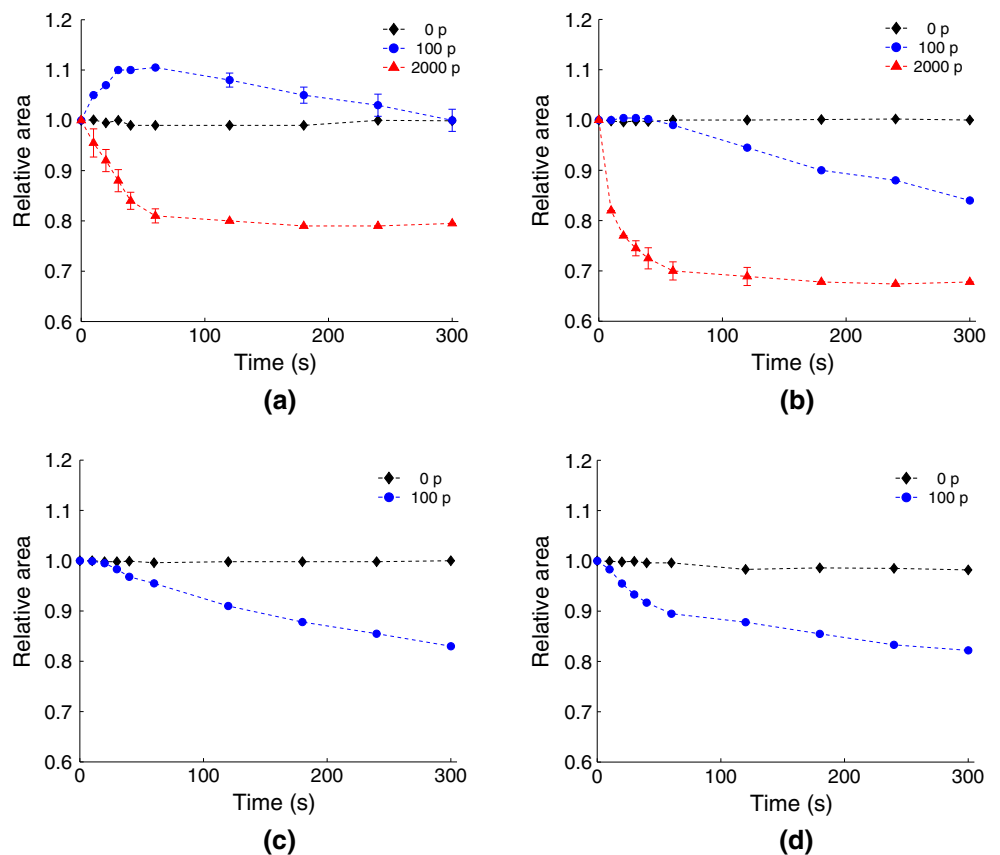
Fig. 6 Cell shrinking in isosmotic media with **a** 150 mOsm/kg and **b** 200 mOsm/kg of sucrose after exposure to 5 ns permeabilizing electropulses (10 MV/m, 1 kHz repetition rate) shows that sucrose remains impermeant at high pulse counts. Results are presented as mean \pm SE for at least 60 cells from at least three independent experiments for each pulsing condition at 25 °C



However, at a lower osmolality of PEG 1000, 50 mOsm/kg, where we expect to see swelling, since the extracellular osmolality of PEG 1000 is less than the intracellular osmolality of large, impermeant solutes, we observe for a 100-pulse exposure an initial increase in cell volume followed by shrinking, instead of simple swelling (Fig. 7). When we increase the pulse count further, to 2000, we see no swelling at all, but only a reduction in cell volume (Fig. 7a).

These results could be explained if some of the large intracellular solutes, which remain impermeant after a dose of 30 pulses, are able to pass through the membrane after a 100-pulse exposure, even though the still larger PEG 1000 molecules in the extracellular medium are still blocked. In that case, one might expect to see first a swelling, resulting from the more rapid diffusion of water and small molecules, followed by an osmotic equilibration resulting from the 100-pulse-induced large-molecule leakage (associated with the slower diffusion of the larger molecules) and

Fig. 7 Cell volume changes in isosmotic media containing pore-blocking PEG 1000 after 100 or 2000 pulses (5 ns, 10 MV/m, 1 kHz), with **a** 50 mOsm/kg, **b** 116 mOsm/kg, **c** 150 mOsm/kg, **d** 200 mOsm/kg of PEG 1000. Results are consistent with plasma membrane permeabilization for intracellular large molecules, but not for extracellular PEG 1000. Results are presented as mean \pm SE for at least 60 cells from at least three independent experiments for each pulsing condition at 25 °C



subsequent shrinkage, since the PEG 1000 molecules still cannot diffuse into the cell. When 2000 pulses are delivered instead of 100, the greater extent of the permeabilization and the consequently more rapid outward diffusion of intracellular solutes eliminate the initial swelling observed with the lower pulse dose.

With a smaller osmotic differential at 116 mOsm/kg of PEG 1000, the initial pulse-induced swelling does not occur with either 100 or 2000 pulses (Fig. 7b). As with 50 mOsm/kg PEG 1000, as the large intracellular solutes leak out of the cell, decreasing the intracellular osmolality, water diffuses outward as well, and the cell shrinks. In all these cases, the membrane remains impermeant to PEG 1000, but the evidence can be interpreted to indicate that at larger pulse exposures, some permeabilizing structures (which may or may not be pores) permit intracellular solutes larger than sucrose, but not as large as PEG 1000, to pass through the membrane.

These results show that PEG 1000 remains impermeant even after cells are exposed to 2000 pulses, 5 ns. From this observation, we infer that there is no significant amount of permeabilizing structures created by 2000 pulses, 5 ns sufficiently large to allow the passage of molecules as large as PEG 1000.

Discussion

Colloidal osmotic imbalance-driven changes in cell volume are a sensitive indicator of nsPEF-induced cell membrane permeabilization, even for pulses as short as 5 ns (André et al. 2010; Romeo et al. 2013). Previously, it has been shown for pulses of much longer duration—60 and 600 ns—that blocking electropermeabilization-induced colloidal osmotic swelling can be used to determine the mean population size of the electropermeabilizing structures (assumed to be lipid electropores) by adding to the external medium molecules that are larger than the size of the electropores (thus balancing the colloidal osmotic pressure of the large intracellular solutes which are unable to pass through the electropermeabilized membrane). As a result, even though we do not have direct evidence for the size of membrane electropores, we can estimate an upper limit on pore size from the diameter of the molecules which block osmotic swelling and therefore are too large to pass through the pores (Nesin et al. 2011). In this work, we employed this method to examine the size of the electropores and the extent of permeabilization in cell membranes exposed to 5 ns, 10 MV/m electric pulses delivered with a 1 kHz repetition rate.

Since both inositol and sucrose block swelling after exposure to 5 pulses, 5 ns, we can conclude that the permeabilizing structures created under these conditions do

not allow transport of either molecule. In other words, these structures must have an effective diameter <0.7 nm (Fig. 5). For 10–30 pulses, cell swelling was blocked by sucrose (0.9 nm) but not by inositol (0.7 nm) (Fig. 5), indicating that a pulse dose in this range produces pores with an effective diameter >0.7 nm but <0.9 nm. Sucrose blocks swelling even with doses as high as 100 pulses, indicating that pore diameter even with this large, multiple-pulse exposure remains <0.9 nm (Fig. 6). If pores larger than 0.9 nm are produced, we can conclude from this data that they are a small fraction of the pore population, since their contribution to the volume change cannot be detected in our measurements. These estimates are consistent with what was reported previously for much longer pulses of duration of 60 and 600 ns (Nesin et al. 2011).

The results summarized in Fig. 5 show that with isosmotic inositol in the medium, the swelling rate, that is the positive rate of change in cell size with time, increases with the number of pulses delivered. This could indicate either that the number of inositol-permeable pores increases with the number of pulses, or that the mean diameter of a population of initially inositol-impermeant pores is increased by the application of multiple pulses. Since our data show that sucrose remains impermeant under these conditions, we consider it unlikely that the diameter of the pores is significantly increased by multiple pulses and more likely that additional inositol-permeant pores are being created.

To explore further the possibility that pore diameter is increased by multiple pulses, we applied a much larger dose—2000 pulses—to cells in isosmotic solutions containing 50 and 116 mOsm/kg PEG 1000 (Fig. 7a, b). Cell volume began to decrease immediately after pulse exposure, and the cells continued to shrink for at least 5 min. This finding seems to be inconsistent with the swelling triggered by 100 pulses applied to suspensions containing 50 mOsm/kg PEG 1000. We hypothesize that a 2000-pulse dose opens pores smaller than PEG 1000 but large enough to permit efflux of the intracellular solutes which are smaller than PEG 1000 but which remain impermeant after a 100-pulse dose. Diffusion-driven equilibration of the intracellular and extracellular osmolalities of these normally impermeant species leaves the still impermeant and extracellular PEG 1000 molecules as the remaining significant osmolytes. To balance the osmotic pressure, water flows out of the cells, causing them to shrink. Also, the effect of 200 mOsm/kg PEG 1000, with respect to 116 and 150 is more evident in terms of rate of shrinking than in the extent of reduction of cells area. The delay of shrinking in Fig. 7b and c may indicate an evolution of the pore population within the first 100 s, resulting in an increase in effective pore size and the leakage of large intracellular solutes that are still smaller than PEG 1000.

Conclusion

We have used inositol, sucrose, and PEG 1000, and the osmotic swelling response to membrane permeabilization to estimate the size of the permeabilizing structures (pores) created by 5 ns, 10 MV/m electric pulses. By this analysis, exposures up to 100 pulses enable the transportation of molecules with a diameter between 0.7 and 0.9 nm. Cell swelling can be prevented by isosmotic PEG 1000 in the external medium with pulse counts up to 2000, indicating that the pore diameter even after this extreme exposure is still smaller than the size of PEG 1000 (about 1.9 nm, assuming that the hydrodynamic radius of PEG 1000 is equivalent to the Einstein–Stokes radius, which is 0.95 nm). It is not possible to determine with the method used in this work the distribution of sizes in the population of pores created by the electric pulse exposures, and for this reason, it cannot be excluded that smaller pores (diameter <0.7 nm) are created along with pores in the 0.7–0.9 nm range. This method of determination will require a careful calibration of transport rates for the various solutes as a function of pore cross section and then an accurate measurement of the flux observed experimentally.

Acknowledgments EBS and PTV received support from the Frank Reidy Research Center for Bioelectrics at Old Dominion University and from the Air Force Office of Scientific Research (FA9550-15-1-0517, FA9550-14-1-0123).

Compliance with Ethical Standards

Conflict of Interest The authors declare that they have no conflict of interest.

References

- André FM, Rassokhin MA, Bowman AM, Pakhomov AG (2010) Gadolinium blocks membrane permeabilization induced by nanosecond electric pulses and reduces cell death. *Bioelectrochemistry* 79:95–100
- Armstrong JK, Wenby RB, Meiselman HJ, Fisher TC (2004) The hydrodynamic radii of macromolecules and their effect on red blood cell aggregation. *Biophys J* 87:4259–4270
- Beebe SJ, Blackmore PF, White J, Joshi RP, Schoenbach KH (2004) Nanosecond pulsed electric fields modulate cell function through intracellular signal transduction mechanisms. *Physiol Meas* 25:1077
- Bilka AO, DeBruin KA, Krassowska W (2000) Theoretical modeling of the effects of shock duration, frequency, and strength on the degree of electroporation. *Bioelectrochemistry* 51:133–143
- Bowman A, Nesin O, Pakhomova O, Pakhomov A (2010) Analysis of plasma membrane integrity by fluorescent detection of TI + uptake. *J Membr Biol* 236:15–26. doi:10.1007/s00232-010-9269-y
- Claessens M, Leermakers FAM, Hoekstra FA, Stuart MAC (2008) Osmotic shrinkage and reswelling of giant vesicles composed of dioleoylphosphatidylglycerol and cholesterol. *Biochim Biophys Acta Biomembr* 1778:890–895
- Craviso GL, Chatterjee P, Maalouf G, Cerjanic A, Yoon J, Chatterjee I, Vernier PT (2009) Nanosecond electric pulse-induced increase in intracellular calcium in adrenal chromaffin cells triggers calcium-dependent catecholamine release. *Dielectr Electr Insul IEEE Trans* 16:1294–1301
- DeBruin KA, Krassowska W (1999) Modeling electroporation in a single cell. I. Effects of field strength and rest potential. *Biophys J* 77:1213–1224
- Garon EB, Sawcer D, Vernier PT, Tang T, Sun Y, Marcu L, Gundersen MA, Koeffler HP (2007) In vitro and in vivo evaluation and a case report of intense nanosecond pulsed electric field as a local therapy for human malignancies. *Int J Cancer* 121:675–682. doi:10.1002/ijc.22723
- Golzio M, Mora M-P, Raynaud C, Delteil C, Teissié J, Rols M-P (1998) Control by osmotic pressure of voltage-induced permeabilization and gene transfer in mammalian cells. *Biophys J* 74:3015–3022
- Kinosita K Jr, Tsong TY (1977) Formation and resealing of pores of controlled sizes in human erythrocyte membrane. *Nature* 268:438–441
- Kuga S (1981) Pore size distribution analysis of gel substances by size exclusion chromatography. *J Chromatogr A* 206:449–461
- Levine ZA, Vernier PT (2010) Life cycle of an electropore: field-dependent and field-independent steps in pore creation and annihilation. *J Membr Biol* 236:27–36. doi:10.1007/s00232-010-9277-y
- Napotnik TB, Wu Y-H, Gundersen MA, Miklavcic D, Vernier PT (2012) Nanosecond electric pulses cause mitochondrial membrane permeabilization in Jurkat cells. *Bioelectromagnetics* 33:257–264. doi:10.1002/bem.20707
- Nesin OM, Pakhomova ON, Xiao S, Pakhomov AG (2011) Manipulation of cell volume and membrane pore comparison following single cell permeabilization with 60- and 600-ns electric pulses. *Biochim Biophys Acta Biomembr* 1808:792–801
- Nuccitelli R, Chen X, Pakhomov AG, Baldwin WH, Sheikh S, Pomicter JL, Ren W, Osgood C, Swanson RJ, Kolb JF (2009) A new pulsed electric field therapy for melanoma disrupts the tumor's blood supply and causes complete remission without recurrence. *Int J Cancer* 125:438–445
- Pakhomov AG, Bowman AM, Ibey BL, Andre FM, Pakhomova ON, Schoenbach KH (2009) Lipid nanopores can form a stable, ion channel-like conduction pathway in cell membrane. *Biochem Biophys Res Commun* 385:181–186
- Pakhomov AG, Gianulis E, Vernier PT, Semenov I, Xiao S, Pakhomova ON (2015) Multiple nanosecond electric pulses increase the number but not the size of long-lived nanopores in the cell membrane. *Biochim Biophys Acta* 1848:958–966. doi:10.1016/j.bbame.2014.12.026
- Rogers WR, Merritt JH, Comeaux J, Kuhnelt CT, Moreland DF, Teltchik DG, Lucas JH, Murphy AR (2004) Strength-duration curve for an electrically excitable tissue extended down to near 1 nanosecond. *Plasma Sci IEEE Trans* 32:1587–1599
- Romeo S, Wu Y-H, Levine ZA, Gundersen MA, Vernier PT (2013) Water influx and cell swelling after nanosecond electropermeabilization. *Biochim Biophys Acta* 1828:1715–1722. doi:10.1016/j.bbame.2013.03.007
- Rubinsky B (2007) Irreversible electroporation in medicine. *Technol Cancer Res Treat* 6:255–259
- Sabirov RZ, Okada Y (2004) Wide nanoscopic pore of maxi-anion channel suits its function as an ATP-conductive pathway. *Biophys J* 87:1672–1685
- Sanders JM, Kuthi A, Wu Y-H, Vernier PT, Gundersen M (2009) A linear, single-stage, nanosecond pulse generator for delivering intense electric fields to biological loads. *Dielectr Electr Insul IEEE Trans* 16:1048–1054

- Saulis G, Venslauskas MS, Naktinis J (1991) Kinetics of pore resealing in cell membranes after electroporation. *Bioelectrochemistry Bioenerg* 26:1–13
- Schoenbach KH, Hargrave B, Joshi RP, Kolb JF, Nuccitelli R, Osgood C, Pakhomov A, Stacey M, Swanson RJ, White J (2007) Bioelectric effects of intense nanosecond pulses. *Dielectr Electr Insul IEEE Trans* 14:1088–1109
- Smith KC, Weaver JC (2011) Transmembrane molecular transport during versus after extremely large, nanosecond electric pulses. *Biochem Biophys Res Commun* 412:8–12. doi:[10.1016/j.bbrc.2011.06.171](https://doi.org/10.1016/j.bbrc.2011.06.171)
- Son RS, Gowrishankar TR, Smith KC, Weaver JC (2016) Modeling a conventional electroporation pulse train: decreased pore number, cumulative calcium transport and an example of electrosensitization. *IEEE Trans Biomed Eng* 63:571–580
- Sukhorukov VL, Imes D, Woellhaf MW, Andronic J, Kiesel M, Shirakashi R, Zimmermann U, Zimmermann H (2009) Pore size of swelling-activated channels for organic osmolytes in Jurkat lymphocytes, probed by differential polymer exclusion. *Biochim Biophys Acta Biomembr* 1788:1841–1850
- Vernier PT, Sun Y, Marcu L, Salemi S, Craft CM, Gundersen MA (2003) Calcium bursts induced by nanosecond electric pulses. *Biochem Biophys Res Commun* 310:286–295
- Vernier PT, Sun Y, Gundersen MA (2006) Nanoelectropulse-driven membrane perturbation and small molecule permeabilization. *BMC Cell Biol* 7:37. doi:[10.1186/1471-2121-7-37](https://doi.org/10.1186/1471-2121-7-37)
- Wu Y-H, Arnaud-Cormos D, Casciola M, Sanders JM, Leveque P, Vernier PT (2013) Moveable wire electrode microchamber for nanosecond pulsed electric-field delivery. *IEEE Trans Biomed Eng* 60:489–496. doi:[10.1109/TBME.2012.2228650](https://doi.org/10.1109/TBME.2012.2228650)
- Zhang J, Blackmore PF, Hargrave BY, Xiao S, Beebe SJ, Schoenbach KH (2008) Nanosecond pulse electric field (nanopulse): a novel non-ligand agonist for platelet activation. *Arch Biochem Biophys* 471:240–248
- Zimmermann U (1982) Electric field-mediated fusion and related electrical phenomena. *Biochim Biophys Acta Rev Biomembr* 694:227–277